



Recycling of iron oxide waste by carbothermic reduction to utilize in FDM 3D printing materials

Korbkaroon DOUNGKEAW¹, Peeraphat SUTTIPONG¹, Phachai KUNGWANKRAI¹, Suksan MUENGTTO¹, Boonlom THAVORNYUTIKARN², and Jennarong TUNGTRONGPAIROJ^{1,*}

¹ Department of Materials and Production Technology Engineering, Faculty of Engineering, King Mongkut's University of Technology North Bangkok, Bangkok 10800, Thailand

² Personalized Devices Research Team, Biofunctional Materials and Devices Research Group, The National Metal and Materials Technology Center (MTEC), The National Science and Technology Development Agency (NSTDA), 114 Thailand Science Park, Phahonyothin Road, Khlong Nueng, Khlong Luang, Pathum Thani 12120, Thailand

*Corresponding author e-mail: jennarong.t@eng.kmutnb.ac.th

Received date:
1 January 2023
Revised date
15 March 2023
Accepted date:
24 March 2023

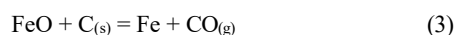
Keywords:
Reduced iron;
Waste;
ABS composite;
3D printing;
Filament

Abstract

Iron oxide scale generally forms on low-carbon steel surfaces during the hot rolling processes and produces as solid waste more than 100 thousand tons per year. The utilization of the iron oxide scale is one possible way to reduce the production cost for steel plants and promote environmental protection. Acrylonitrile-Butadiene-Styrol-Copolymer (ABS) is widely used as engineering plastic for automotive parts because of its high strength and wear resistance. The recycling of iron oxide waste as reinforcement particles for enhancing the tensile strength of ABS composite was studied. The iron oxides were recycled by carbon powder at a high temperature between 1150°C to 1350°C up to 120 min. After the reduction process, the reduced iron from an optimal condition with the iron-rich fraction was ground to powder. Afterward, the 0.3 vol% to 1.3 vol% powders were mixed with ABS polymer powder and formed as composite filaments for additive manufacturing (FDM 3D printing). The tensile strength of pure ABS filament increased to 37.16 ± 2.37 MPa when added recycled iron powders. The regular distribution and 13.68 ± 9.78 μm of recycled-iron particle sizes on the ABS matrix were investigated and correlated to the mechanical properties.

1. Introduction

In hot rolling processes, low carbon steel slabs are heated over 1000°C for deformation and produced into steel strips [1]. The oxidation of steel can take place and generate iron oxide scale on the steel surfaces, which is mostly removed as manufacturing waste after the process. Moreover, iron oxide waste is generally recycled as raw materials in steelmaking processes, industrial pigments, and additives for battery electrolyte solutions [2]. Hematite (Fe_2O_3) and Magnetite (Fe_3O_4) are mainly chemical compounds in iron oxide scales. In a reduction reaction, they can be recycled to Fe by reducing agents such as solid carbon and carbon monoxide [3]. The reduction can start at a temperature above 800°C for the indirect reaction and 1000°C for the direct reaction, as shown in Equation (1-3).



The work of O. Benchiheb *et al.* reported the chemical composition of raw iron oxide waste with a diameter of 10 mm to

16 mm from a hot rolling mill composed of Fe_2O_3 , Fe_3O_4 , and FeO [4]. They were reduced using mixed CO/N_2 gas between 40% to 60% CO at 750°C to 1050°C for 40 min to 180 min. The reduction rate of oxide waste increased when the particle size decreased and the reduction temperature, time, and fraction of CO increased. The Fe and Fe_3C were generated after the reduction at 750°C, but the Fe_3C disappeared after heating to 850°C. Besides, the pure iron was only presented after the reduction at 1050°C. The reduction temperature played an essential role in producing porous reduced iron at high temperatures and whisker iron at low temperatures [5]. The reduced iron from the reduction process can be further applied to powder metallurgy (PM) processes [6] to produce many industrial applications, such as brake pads in automobile parts [7].

3D-printing technology or additive manufacturing (AM) is a new forming process and has become disruptive technology replacing standard manufacturing processes such as stamping and forging. This forming method can make near-net shapes and complex products through rapid and low-cost production with a low workforce. Several materials, e.g., metal, polymer, ceramic, and composite materials, can be printed by 3D-printing technology [8-11]. Polymer-matrix composites (PMCs) are composite materials that mix between polymer matrix and reinforcement,

such as metal particles or fibers. The PMCs are lightweight and have a higher strength-to-weight ratio than other materials. It is mostly used to make automotive, railway, and aerospace parts [12]. The additive manufacturing of PMCs commonly uses the fused filament fabrication (FFF) method, also known as fused deposition modeling (FDM), in the trademark name. The 3D printing of PMCs filament of ABS reinforced by CuFe_2O_4 (copper ferrite) and ZnFe_2O_4 (Zinc ferrite) was studied [13,14]. The more weight percentage of reinforcement particles tended to increase the tensile strength and thermal conductivity but decrease elongation at break. Besides, the tensile strength of thermoplastic composites (Carbon fiber reinforced plastic, CFRP) was improved to 42 MPa when topped up with the carbon fiber with an average length of 150 μm at 5 wt% [15]. Furthermore, the high percentage of reinforcing aluminum filler increased the wear resistance of Nylon composite materials [16]. However, the friction coefficient of ABS composites remarkably decreased with filling graphite powders [17]. The irregular morphology of 30 mm-stainless steel powder was used to improve interfacial interactions between reinforcing stainless-steel particles and the polymer matrix because of increasing surface roughness and mechanical interlocking [18]. Moreover, the reinforcement of copper particles can promote the thermal conductivity of ABS/Cu composite filament, and the property increases when increasing the copper content [19].

In this work, the recycling of iron oxide scale using carbothermic reduction with graphite powders was observed and utilized as reinforcing fillers in ABS composite materials for 3D printing technology. The reduction of iron oxide was analyzed by mass change measurements before and after the reduction test and phase analysis using an X-ray diffractometer (XRD). Finally, the physical characterization and mechanical properties of the composites, e.g., melt flow rate and tensile strength, were investigated.

2. Experimental

2.1 Carbothermic reduction test

The iron oxide waste was prepared in a diameter of 4 cm to 5 cm and dried in an oven at a temperature below 200°C for an hour. Afterward, the iron oxide scale was split to a small size with a one-cm diameter. The weight and size of the iron oxide scale were measured by an electronic analytical balance of 0.0001 g and a vernier caliper,

respectively. Then the prepared oxide samples were covered with graphite powders in a crucible and heated in a horizontal tube furnace at 1150°C to 1350°C for 15 min to 120 min. During the carbothermic reduction, the closed graphite packing system was shielded by argon gas with a one-litter-per-hour flow rate.

After the test, the samples were weighed, and analyzed the chemical compound by XRD (SmartLab). The XRD analysis was conducted with the incident Cu-K α line, $\lambda = 1.5406 \text{ \AA}$, at 40 kV and 40 mA, and the range angle $2\theta = 20$ to 80 degrees (sampling width of 0.02 degree). The reduced iron containing a high percentage of iron was selected to grind by mechanical ball milling and sieved to a size of less than 40 μm .

2.2 Polymer composite extrusion

The optimum reduced iron powder from the previous section was mixed with commercial ABS powder (Melt flow index; 7 g/10 min) from IRPC Public Company Limited, Thailand, and the mean size of ABS powder is 1 mm, as shown in Figure 2(a) and Figure 2(b). The reduced iron powder was mixed in the ABS matrix powder of 25 g at 0.564, 0.942, 1.894, and 2.469 g following the mixing equation in Equation (4) and showed the corresponding volume percentages of 0.3, 0.5, 1.0, and 1.3 vol% in Table 1. Subsequently, the two mixed powders were extruded into polymer composite filament by a single screw extruder at a strand-die temperature of 220°C to 230°C to produce a 1.75 mm filament, as shown in Figure 2(c).

The extruded polymer composite filaments of ABS and reduced iron particles were characterized using an optical microscope and a scanning electron microscope (SEM) (FEI QUANTA 450, Austria) equipped with energy dispersive spectroscopy (EDS) with an EDAX (Singapore) EDS detector at 15 keV. The melt flow rate (MFR) of the composite was tested by Melt Index Tester (KARGE Industrietechnik) according to ASTM D 1238-20. Furthermore, the mechanical tests were applied, i.e., tensile test (Cometech; QC-506M) following ASTM-D2256 (Yarns tensile testing; overall length: 150 mm, speed: 10 mm·min⁻¹) and hardness test (Shore D hardness tester with an indenter tip radius of 0.100 \pm 0.012 mm, Rex durometer Model OS-1) following ASTM D2240.

$$V_r = \frac{M_r/\rho_r}{(M_r/\rho_r) + (M_m/\rho_m)} \quad (4)$$

where V = volume, M = mass (g), r = reinforcement, m = matrix, ρ = density ($\text{g}\cdot\text{cm}^{-3}$), density of ABS ($\rho_{\text{ABS}} = 1.01 \text{ g}\cdot\text{cm}^{-3}$), and density of reduced iron ($\rho_{\text{Fe}} = 55.85 \text{ g}\cdot\text{cm}^{-3}$).

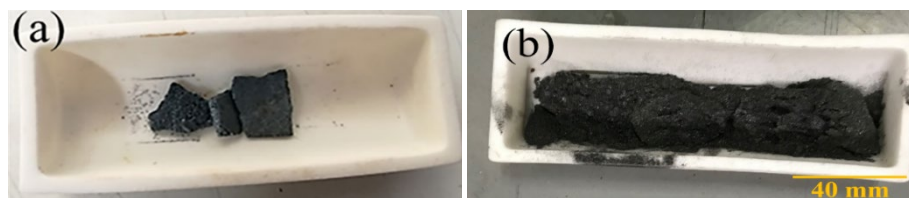


Figure 1. Prepared iron oxide samples in a crucible (a) before and (b) after the carbothermic reduction test.

Table 1. The volume fraction of reduced iron and ABS at different volume percentages.

Composite materials	Weight content			
	0.3 vol%	0.5 vol%	1.0 vol%	1.3 vol%
Reduce iron	0.564 g	0.942 g	1.894 g	2.469 g
ABS	25 g	25 g	25 g	25 g

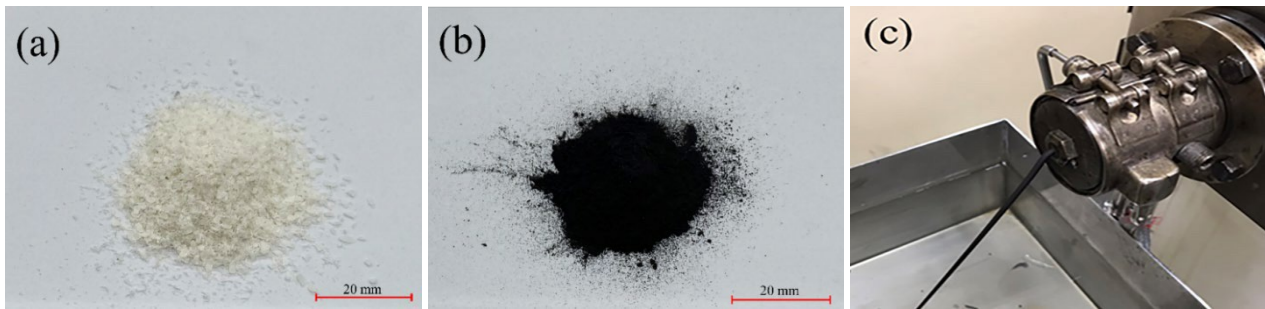


Figure 2. (a) ABS powder, (b) reduced iron powder, and (c) polymer.

3. Results and Discussion

3.1 Weight loss after carbothermic reduction

The weight loss of iron oxide samples after the carbothermic reduction test is presented in Figure 3. The weight loss seemingly increased when increased the reduction temperature and prolonged time, which means the iron oxide can be changed to iron and oxygen is removed according to Equation (1-3). This result is related to the previous work that the iron oxide was extracted into pure iron by a reduction process with 40% to 60% CO-balance N₂ at 750°C to 1050°C for 40 min to 180 min [4]. The oxide sample at 1350°C presented a high weight loss at every reduction time. Thus, the reduction at 1350°C was selected as an optimum condition for reducing iron in this work. After the test and grinding into powders, the reduced iron particles presented an irregular shape (Figure 4), and the average diameter was $13.68 \pm 9.78 \mu\text{m}$. The XRD analysis was carried out to reveal the chemical composition of reduced iron after the test at 1350°C for 15 min to 120 min, as illustrated in Figures 5 and Figure 6. The as-received oxide before the test showed only the peak of hematite (Fe₂O₃), and the peak of iron was primarily found after the reduction for 15 min. At 120 min, there was only the peak of iron which can be concluded that the iron oxide was totally reduced to iron at this period.

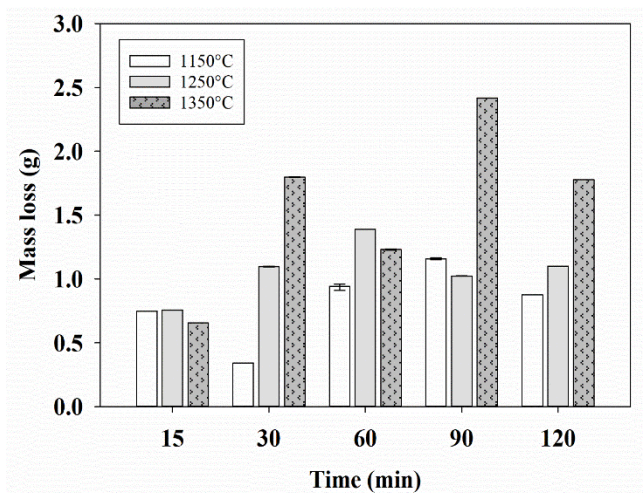


Figure 3. The weight loss of iron oxide scale by carbothermic reduction with solid graphite powder.

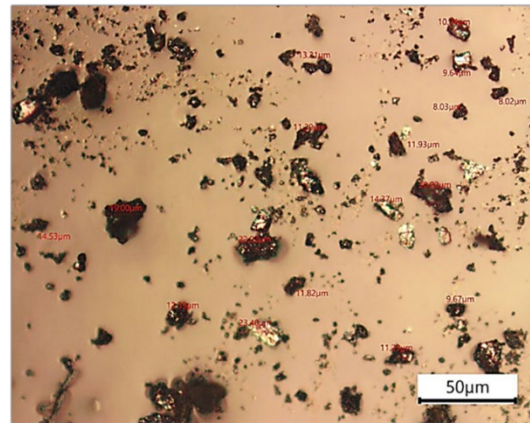


Figure 4. An optical microstructure image of reduced iron particles after the carbothermic reduction test.

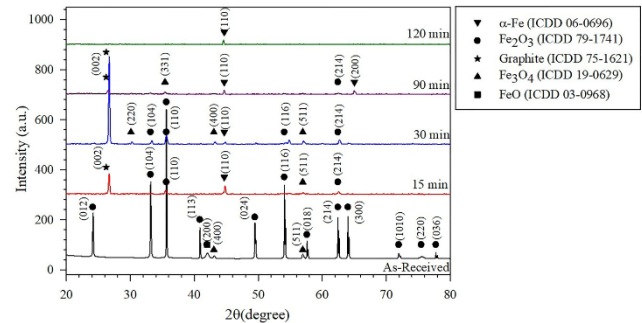


Figure 5. XRD patterns of reduced iron at temperature 1350°C compared to holding times 15, 30, 90, and 120 min.

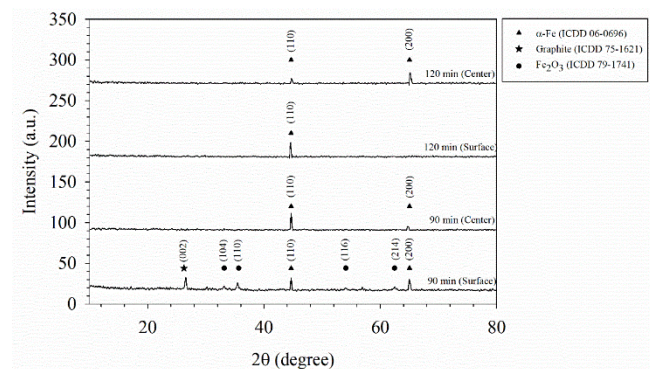


Figure 6. XRD patterns of reduced iron at the center and surface and 1350°C for 90 min and 120 min.

Moreover, the chemical composition of the reduced iron at the center and surface was compared to observe the reduction at different positions. In Figure 6, the peaks of Fe and Fe₂O₃ were detected in the reduced iron sample at the surface for 90 min, but the Fe₂O₃ did not appear at the center. Only the peak of Fe can be found for 120 min at both positions. For this reason, the iron oxide can be completely reduced to iron at the reduction temperature of 1350°C for 120 min.

3.2 Physical properties and characterization of polymer matrix composite

After the carbothermic reduction, the reduced iron samples from the optimum condition were taken to grind and sieve to a small size of less than 40 μm. The reduced iron powders were mixed with ABS powder to form PMC filaments at 0.3, 0.5, 1.0, and 1.3 vol%, and the average diameter of the composite filament is 1.74 ± 0.26 mm, as shown in Figure 7(a). The melt flow rate of ABS composite, when applied with a standard load of 5 kg, was slightly lower than that of the pure ABS at the temperature between 240°C to 250°C (Figure 7(b)). Nevertheless, the melt flow of both materials was significantly different

when increased the temperature more than 250°C. This behavior can indicate that the forming and printability of the ABS composite are a bit lower than the pure ABS. However, it is the typical behavior of polymer composite compared to pure polymer grades. Concerning the cross-sectional microstructure in the longitudinal direction of the ABS composite filament presented in Figure 8, the reduced iron particles distributed and existed as a white phase on the ABS matrix (gray phase). Besides, the fraction of reduced iron particles in the pictures was estimated by ImageJ software and around 0.34, 0.51, 1.01, and 1.28 %area at 0.3, 0.5, 1.0, and 1.3 vol% reduced iron, respectively. Consequently, the area fraction of reduced iron in ABS composite is close to the volume fraction in the experimental setup.

The morphology and distribution of reduced iron particles on the cryogenic liquid nitrogen fracture surface of ABS composite were further observed by SEM, as shown in Figure 9(a). The irregular spherical shape of reduced iron was revealed, and the EDS points analysis showed Fe peak in the reduced iron particle (point 1), as presented in Figure 9(b). It is noted that the peaks of carbon and oxygen in the EDS spectrum possibly were from contaminants during carbothermic reduction.

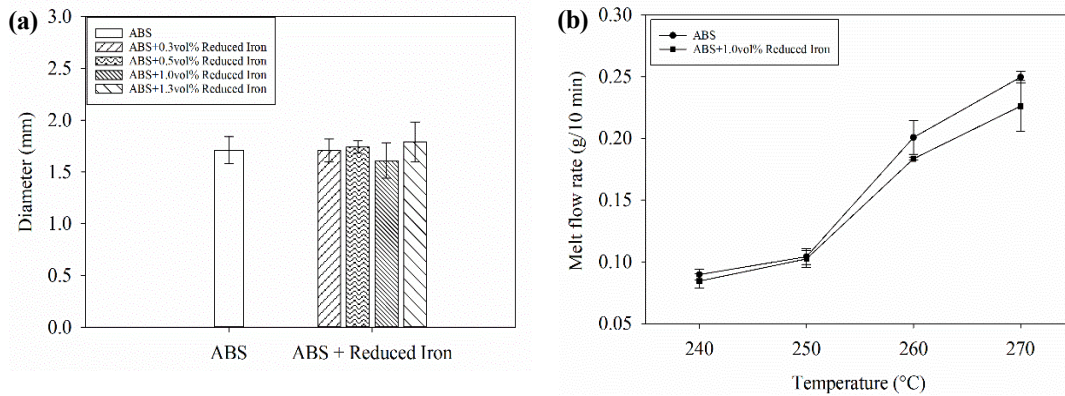


Figure 7. Physical properties of ABS composite with reduced iron particles (a) diameter (b) melt flow rate.

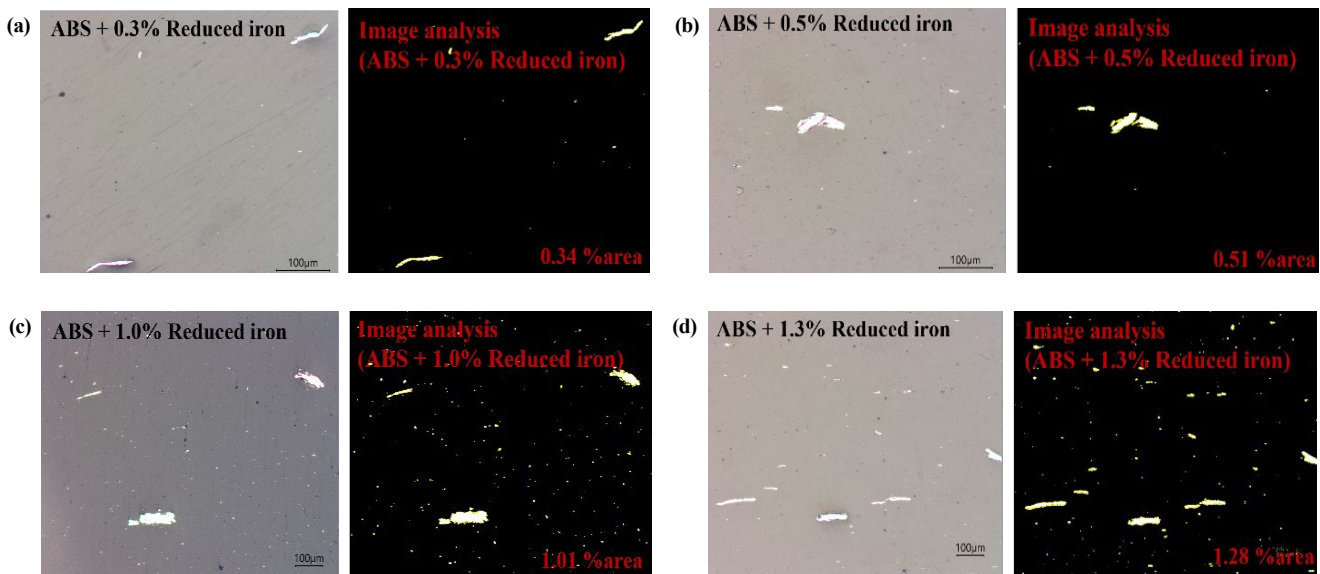


Figure 8. Optical microstructure images and image analysis of ABS composite filament with different percentages of reduced-iron reinforcement particles (a) 0.3 %area, (b) 0.5 %area, (c) 1.0 %area, and (d) 1.3 %area.

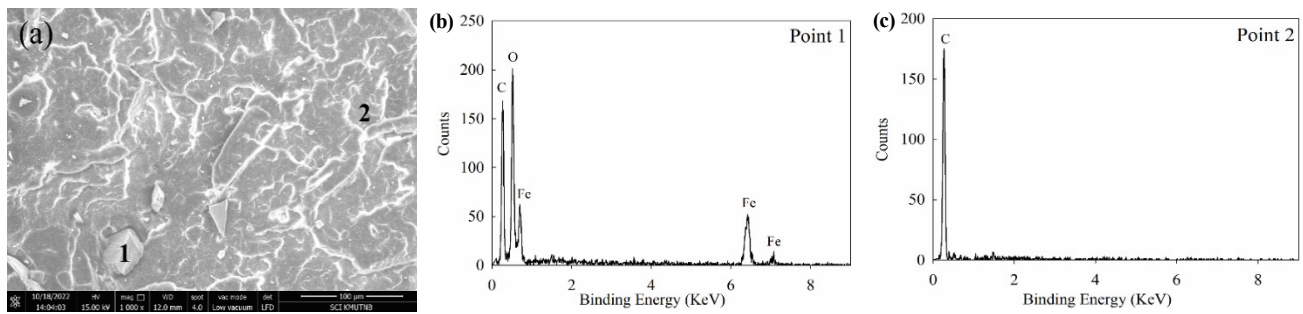


Figure 9. An SEM image of a cryogenic liquid nitrogen fracture surface of (a) the ABS+1.0 vol% Reduced iron, (b) and (c) EDS elemental spectra of the point 1 and 2.

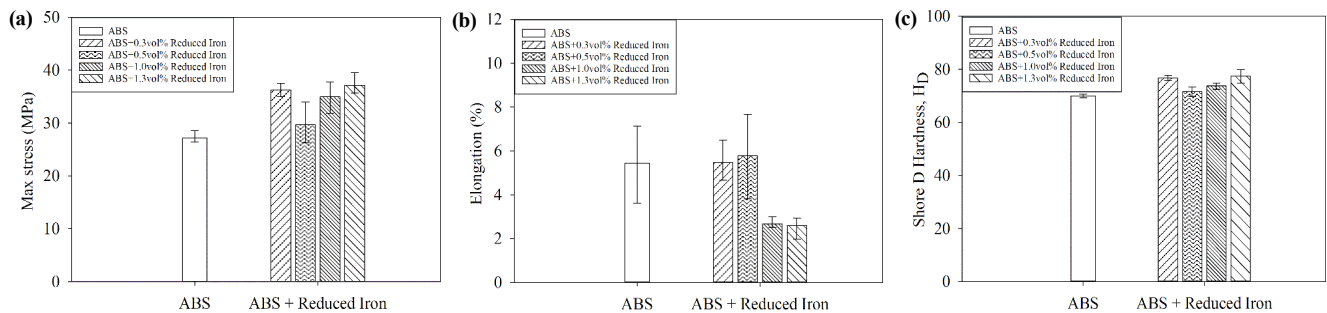


Figure 10. Mechanical properties of ABS composite filament at different volume percentages of reduced iron particles (a) max stress, (b) elongation at break, and (c) hardness.

3.2 Mechanical properties

The tensile property of the ABS composite filament at different reduced-iron ratios was determined according to the ASTM-D2256 and presented as max stress in Figure 10. The max stress was improved with increasing the fraction of reduced iron, and the highest max stress was around 37.16 MPa at 1.3 vol%. The stress-strain curve of an ABS composite filament with the highest max stress at 1.3 vol% compared with a pure ABS one is presented in Figure 11. On the contrary, the elongation at break tended to decrease when the reduced iron ratio increased. These results agree with the mechanical properties of common polymer composite materials with a higher strength but lower elongation percentage than polymers [20,21]. The hardness of ABS composite was not insignificantly changed at different percentages of reduced iron, and the average hardness was 75.09 ± 0.41 Hb.

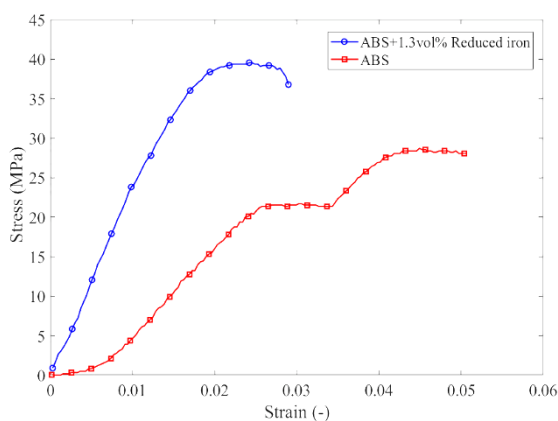


Figure 11. Stress-strain curves of ABS composite at 1.3 vol% reduced iron and compared with the pure ABS filament.

4. Conclusion

Iron oxide waste from steel industries can be recycled by carbothermic reduction and used as reinforcements in ABS composites. The iron oxide scale started to reduce at a temperature above 1150°C for 15 min. Furthermore, the optimum carbothermic reduction with graphite powders for converting iron oxide waste to iron was at 1350°C for 120 min. Fine irregular reduced iron particles appeared after the powder preparation, and they presented irregular spherical shapes on the cross-sectional microstructure of ABS composite filament after polymer extrusion. Moreover, the melt flow rate associated with the 3 D printability of the ABS composite was slightly lower than that of pure ABS. The tensile strength of the ABS composite increased as the percentage of reduced iron increased, and the highest max stress showed around 37.16 MPa at 1.3 vol% reduced iron. However, the percent elongation at break insignificantly decreased.

Acknowledgements

This work was supported by the National Research Council of Thailand (NRCT), Graduate Study Development Grant (2023) and kindly technical supported by the National Metal and Materials Technology Center (MTEC), the National Science and Technology Development Agency (NSTDA).

References

- [1] V. B. Ginzburg, Flat-Rolled Steel Processes (Advanced Technologies), CRC Press, 2009.

- [2] B. T. Hang and T. T. Anh, "Controlled synthesis of various Fe₂O₃ morphologies as energy storage materials," *Scientific Reports*, vol. 11, pp. 5185, 2021.
- [3] A. Babich, D. Senk, and H.W. Gudenau, *Ironmaking, Stahleisen*, Düsseldorf, 2016.
- [4] O. Benchiheub, S. Mechachti, S. Serrai, and M. G. Khalifa, "Elaboration of iron powder from Mill scale," *Journal of Materials and Environmental Science*, vol. 1, no. 4, pp. 267-276, 2010.
- [5] M. C. Bagatini, V. Zymła, E. Osório, and A. C. F. Vilela, "Characterization and reduction behavior of mill scale," *ISIJ International*, vol. 51, no. 7, pp. 1072-1079, 2011.
- [6] K. S. Sista, and S. Dwarapudi, "Iron powders from steel industry by-products," *ISIJ International*, vol. 58, no. 6, pp. 999-1006, 2018.
- [7] S. N. Nagesh, C. Siddaraju, S. V. Prakash, and M. R. Ramesh, "Characterization of brake pads by variation in composition of friction materials," *Procedia Materials Science*, vol. 5, pp. 295-302, 2014.
- [8] C. Suwanpreecha, S. Songkuea, S. Linjee, S. Muengto, M. Bumrungron, and A. Manonukul, "Tensile and axial fatigue properties of AISI 316L stainless steel fabricated by materials extrusion additive manufacturing," *Materials Today Communications*, vol. 35, 2023.
- [9] J. Surisaeng, W. Kanabenja, N. Passornprasit, and C. Aumnate, "Polyhydroxybutyrate/polylactic acid blends: An alternative feedstock for 3D printed bone scaffold model," *Journal of Physics: Conference Series*, vol. 2175, 2022.
- [10] B. Thavornnyutikarn, P. Tesavibul, K. Sitthiseripratip, N. Chatarapanich, B. Feltis, P. F. Wright, and T. W. Turney, "Effect of partial pre-sintering on structural and mechanical properties of scaffolds," *Materials Science and Engineering: C*, vol. 75, pp. 1281-1288, 2017.
- [11] K. Sakunphokesup, P. Kongkrekri, A. Pongwisuthiruchte, C. Aumnate, and P. Potiyaraj, "Graphene-enhanced ABS for FDM 3D printing: effects of masterbatch preparation techniques," *IOP Conference Series: Materials Science and Engineering*, vol. 600, 2019.
- [12] P. L. López, *Mechanical characterization of composite materials: fracture energies*, Madrid: Universidad Carlos III de Madrid, Inc., 2018.
- [13] K. A. Hamzah, C. K. Yeoh, M. M. Noor, P. L. Teh, Y. Y. Aw, S. A. Sazali, and W. M. A. W. Ibrahim, "Mechanical properties and thermal and electrical conductivity of 3D printed ABS-copper ferrite composites via 3D printing technique," *Journal of Thermoplastic Composite Materials*, vol. 35, 2019.
- [14] S. S. Aqzna, C. K. Yeoh, M. S. Idris, P. L. Teh, K. A. bin Hamzah, Y. Y. Aw, and T. N. Atqah, "Effect of different filler content of ABS-zinc ferrite composites on mechanical, electrical, and thermal conductivity by using 3D printing," *Journal of Vinyl and Additive Technology*, vol.24, no. S1, pp. E217-E229, 2018.
- [15] F. Ning, W. Cong, J. Qiu, J. Wei, and S. Wang, "Additive manufacturing of carbon fiber reinforced thermoplastic composites using fused deposition modeling," *Composites Part B: Engineering*, vol. 80, pp. 369-378, 2015.
- [16] K. S. Boparai, and R. Singh, and H. Singh, "Wear behavior of FDM parts fabricated by composite material feed stock filament," *Rapid Prototyping Journal*, vol. 22, no. 2, pp. 350-357, 2016.
- [17] B. B. Difallah, M. Kharrat, M. Dammak, and G. Monteil, "Mechanical and tribological response of ABS polymer matrix filled with graphite powder," *Materials & Design*, vol.43, pp. 782-787, 2012.
- [18] M. A. Ryder, D. A. Lados, G. S. Iannacchione, and A. M. Peterson, "Fabrication and properties of novel polymer-metal composites using fused deposition modeling," *Composites Science and Technology*, vol. 158, pp.43-50, 2018.
- [19] S. Hwang, E.I. Reyes, Ks. Moon, R. C. Rumpf, and N. S. Kim, "Thermo-mechanical characterization of metal/polymer composite filaments and printing parameter study for fused deposition modeling in the 3D printing process." *Journal of Electronic Materials*, vol. 44, pp. 771-777, 2015.
- [20] N. Chawla, *Metal Matrix Composite*. United States of America: Springer Science Business Media, Inc., 2006.
- [21] M. Kutz, "Chapter 10 Composite Materials " in *Handbook of Mechanical Engineers*, John Wiley & Sons, Inc., 2015, pp. 401-420.